Original Paper

phys. stat. sol. (b) **244**, No. 3, 1109–1117 (2007) / **DOI** 10.1002/pssb.200642494

ESR study of $La_{1-x}Pb_xMnO_3$ ($0.1 \le x \le 0.5$) perovskites

T. L. Phan[*, 1], **S. G. Min**[2], **M. H. Phan**[3], **N. D. Ha**[4], **N. Chau**[5], and **S. C. Yu**[2]

[1] Nano/Micro Structures Group, Department of Physics, University of Bristol, Bristol BS8-1TL, UK
[2] Department of Physics and BK 21 Physics Program, Chungbuk National University, Cheongju 361-763, Korea
[3] Department of Aerospace Engineering, University of Bristol, BS8-1TR, UK
[4] Department of Materials Engineering, Chungnam National University, Daejeon, 305-764, Korea
[5] Center for Materials Science, University of Natural Science, 334 Nguyen Trai, Hanoi, Vietnam

Received 20 April 2006, revised 1 September 2006, accepted 26 September 2006
Published online 17 November 2006

PACS 75.30.Kz, 75.47.Lx, 76.30.Fc

Electron spin resonance (ESR) spectra of $La_{1-x}Pb_xMnO_3$ ($0.1 \le x \le 0.5$) compounds were recorded at different temperatures. Asymmetrical and distored resonance signals due to ferromagnetic correlations at temperatures $T < T_{min}$ became Lorentzian at $T > T_{min}$, where T_{min} is the temperature corresponding to the narrowest ESR linewidth. The ESR linewidth with respect to temperature, $\Delta H(T)$, for the samples was fitted to the one-phonon process, $\Delta H(T) = A + BT$. We found that B decreased from 5.45 Oe/K for $x = 0.1$ to 4.61 Oe/K for $x = 0.5$, indicating the decrease of lattice distortions with the Pb addition. The temperature dependence of the ESR intensity, $I(T)$, for the samples was described well to an expression of $I(T) = I_0 \exp(E_a/k_BT)$. In the high-temperature region, $1/I(T)$ obeyed the Curie–Weiss law.

1 Introduction

In recent years, the discovery of the so-called colossal magnetoresistance (CMR) effect around the ferromagnetic (FM)-to-paramagnetic (PM) phase transition temperature, T_C, in the hole-doped perovskite manganites system of $R_{1-x}A'_xMnO_3$ (R = La, Pr, Nd; A' = Ca, Sr, Ba, Pb, etc.) has renewed a great deal of interest from research groups [1, 2]. Such interest started from a matter of fact that this material family holds great promises for technological applications, including magnetic sensors, magnetic refrigerators, magnetoresistive-reading heads, and magnetoresistive random access memory. As a function of temperature, magnetic field, doping, applied pressure, the average radius of A-site ions $\langle r_A \rangle$ and A-site size disorder, their electrical and magnetic behaviors are extremely sensitive to those changes, and consequently, these manganites display a phase diagram with enriching magneto-transport properties [1–3]. It is worth to mention that it is possible to modify T_C to a value near and above room temperature, where such practical applications have been realized. Among CMR materials investigated, two systems of Sr- and Pb-doped $La_{1-x}(Sr, Pb)_xMnO_3$ manganites have been found to be the highest T_C values [1–12]. This was explained in detail by Radaelli et al. [3]. It is interesting that $La_{1-x}Pb_xMnO_3$ ($0.1 \le x \le 0.5$) compounds with their T_C values around 300 K could promising potentials for high-temperature applications [4–14].

Historically, $La_{1-x}Pb_xMnO_3$ compounds have been studied since 1970s. At that time, CMR occurring near 300 K was observed in these materials [4–6]. Based on experiments of X-ray and ultraviolet photoemission, Alvarado et al. [5] revealed an existence of the double-exchange conduction band in the FM regime, $T < T_C$. However, such previous works were sparse, not systematical, and only investigated on in

* Corresponding author: e-mail: ptlong2512@yahoo.com, Phone: +82-43-271-8146, Fax: +82-43-274-7811

a narrow range of the x value. Until 1995, the properties of $La_{1-x}Pb_xMnO_3$ compounds with a wide doping range of $0.1 \le x \le 0.5$ was investigated by Mahendiran et al. [7]. It was shown that T_C of the samples investigated was between 300 and 340 K, and at a relatively low-doping level ($x = 0.1$) the CMR value at 300 K was 80% at 6 T [7]. At the same time, Jia et al. [8] also reported that CMR of a $La_{0.6}Pb_{0.4}MnO_3$ single crystal reached a maximum value of 64% at 6 T. Recently, Pb-doped manganite films for magnetic tunnel junctions have been fabricated and studied by Yamada et al. [13]. Obviously, there has been growing interest in $La_{1-x}Pb_xMnO_3$ [11–14] or perovskite manganites doped with Pb [8, 15] and such works have indeed enriched more and more the electrical and magnetic properties of this materials family. Nonetheless, a complete understanding of the internal dynamic properties of the Pb-doped manganites is not yet fulfilled.

In this context, electron spin resonance (ESR) has been proved to be useful for studying spin dynamics of Mn^{3+} and Mn^{4+} ions, interaction mechanisms, and dynamical Jahn–Teller distortions in perovskite manganites around T_C where the CMR effect often observes [16–28]. To the best of our knowledge, no ESR study has been done systematically on $La_{1-x}Pb_xMnO_3$ compounds in a large range of compositions, e.g. $0.1 \le x \le 0.5$. Therefore, we have used ESR to investigate the internal dynamic properties of $La_{1-x}Pb_xMnO_3$ ($0.1 \le x \le 0.5$) polycrystalline manganites in a wide temperature range from around their T_C values to ~500 K. The results obtained provide further understanding of the spin dynamics in Pb-doped manganites.

2 Experiment

$La_{1-x}Pb_xMnO_3$ (x = 0.1, 0.2, 0.3, 0.4, and 0.5) polycrystalline samples were prepared by conventional solid-state reaction. Powder precursors of La_2O_3, PbO, and $MnCO_3$ with a purity of 99.9% were stoichiometrically well-mixed and then pressed into five pellets. The pressed pellets were pre-sintered at 900 °C for 15 hrs, after several intermediate grindings and pressings. Finally, they were sintered at 920 °C for 15 hrs. The samples sintered at high temperatures were slowly cooled down to room temperature. These processes were carried out in the normal atmosphere condition. The quality of the final products was checked by powder X-ray diffraction patterns, D5005-Brucker. Electron spin resonance (ESR) measurements on powdered samples of 20 mg were carried out by a JEOL-TE300 ESR spectrometer operating at 9.2 GHz (X-band) in a temperature range from T_C to ~500 K.

3 Results and discussion

Before carrying out ESR measurements, their Curie temperature (T_C) was determined to be 235, 310 and ~360 K for x = 0.1, 0.2 and $x \ge 0.3$ compositions, respectively, as summarized in Table 1. These results are in good agreement with earlier reports [7–14].

Figure 1 shows ESR signals for the samples at some representative temperatures in the ferromagnetic and paramagnetic phases. As can be seen that asymmetrical and distorted ESR signals at temperatures $T < T_{min}$ become Lorentzian at temperatures $T > T_{min}$, where T_{min} is the temperature corresponding to the narrowest ESR linewidth [4, 17, 20, 30–33]; the average value of T_{min} for the samples is about $1.1T_C$ [19]. Below T_{min}, ESR signals are splitted into two lines [16, 28] corresponding to different resonance positions H_r [H_r is indicated in Fig. 1(f)], as shown in Fig. 2. The first line shifts to low fields with decreasing temperature whereas the second one is temperature independent, excepting for the temperature region $T < \sim 0.87T_{min}$ in that it shifts to higher fields with lowering temperature; this is probably due to influences of localized magnetic moments [19]. Around T_{min}, these lines compete strongly in amplitude, particularly for x = 0.1, 0.2, and 0.5 compositions. However, for x = 0.3 and 0.4 compositions in which the ferromagnetic (FM) phase is dominate, there is the absence of drastic competition in amplitude of the lines near T_{min}. This was evidently reflected by the occurrence of the sharp FM–PM phase transition followed by the large-magnetic-entropy change in these samples [14].

To elucidate changes in ESR signals, we determined the temperature dependences of both the ESR linewidth $\Delta H(T)$ and the peak-to-peak ESR linewidth $\Delta H_{pp}(T)$ for the samples, as defined in Fig. 1(f).

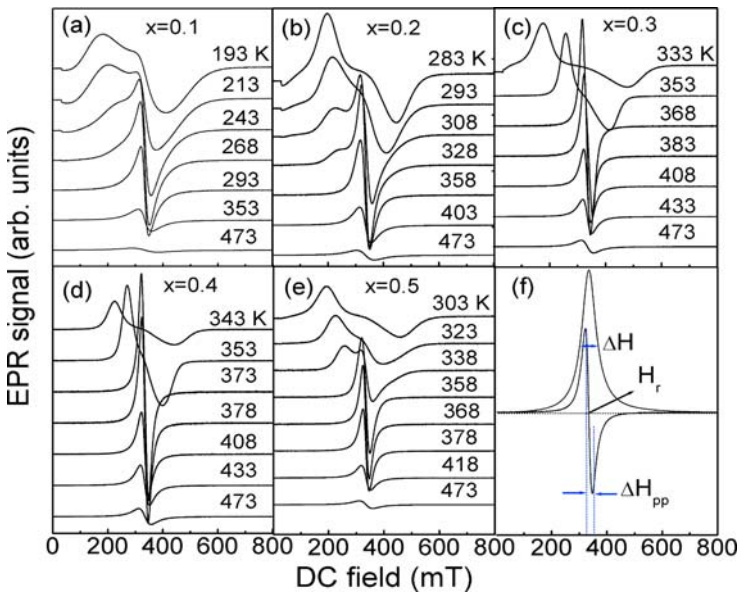

Fig. 1 (online colour at: www.pss-b.com) X-band ESR signals for $La_{1-x}Pb_xMnO_3$ (x = 0.1, 0.2, 0.3, 0.4, and 0.5) compounds at several selected temperatures. Asymmetrical signals or splitting into resonance lines at temperatures $T < T_{min}$ become Lorentzian at $T > T_{min}$, T_{min} values for the samples are summarized in Table 1.

Because of $\Delta H = \sqrt{3}\,\Delta H_{pp}$ [32], we only plot the ΔH data for the samples in Fig. 3(a, b). It should be noticed here that the $\Delta H(T)$ data were obtained by using Eq. (1) to fit ESR signals recorded at different temperatures; this is carried out when the linewidth is of the order of the resonance field [29].

As we can see clearly that ΔH first decreases, then reaches a minimum value ΔH_{min} at T_{min} and finally increases with decreasing temperature, because of development of FM correlations [17, 23]. In the present case, $\Delta H(T)$ considerably decreased as La was substituted by Pb in the doping range of $x = 0.1-0.3$ whereas it increased gradually for further addition of Pb, $x > 0.3$. It is generally known that the ESR linewidth for manganites containing either Mn^{3+} or Mn^{4+} ions individually is larger than that for manganites containing both these ions [18, 23]. Thus, the partial substitution of La by Pb introduces Mn^{4+} ions into the sample. When the ratio of Mn^{3+}/Mn^{4+} reaches 7/3 (x = 0.3), FM correlations are the strongest thereby resulting in the lowest value of $\Delta H(T)$.

$$\frac{dP}{dH} \propto \frac{d}{dH}\left[\frac{\Delta H}{4(H+H_r)^2+\Delta H^2}+\frac{\Delta H}{4(H-H_r)^2+\Delta H^2}\right]. \quad (1)$$

Table 1 Experimental parameters determined for the $La_{1-x}Pb_xMnO_3$ samples, the Curie temperature T_C, the temperature T_{min} where the ESR linewidth is ΔH_{min}, Θ is the Curie–Weiss temperature, and T_L ($> T_{min}$) is a temperature which the theoretical functions fitting well to the experimental data.

x	T_C (K)	T_{min} (K)	T_L (K)	Θ (K)	ΔH_{min} (Oe)	B (Oe/K)	E_{a1} (eV)	E_{a2} (eV)
0.1	235	290	303	274	703	5.45	0.089	0.107
0.2	310	363	368	332	552	5.21	0.093	0.147
0.3	358	382	388	357	376	4.98	0.187	0.194
0.4	360	378	388	353	384	4.80	0.164	0.184
0.5	355	368	373	336	392	4.61	0.128	0.173

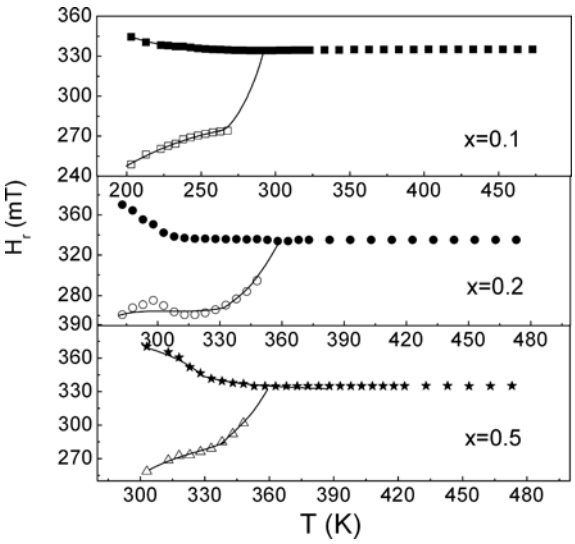

Fig. 2 Plot of H_r for x = 0.1, 0.2 and 0.5 compositions vs. temperature. Solid lines are guides to the eye only. Two lines at $T < T_{min}$ due to the FM correlations become a sole line at $T > T_{min}$, the PM phase.

Concerning the mechanism of the broadening of $\Delta H(T)$ for the samples in the temperature region $T > T_{min}$, it is caused by spin–spin and/or spin–lattice interactions in the one-phonon relaxation process [17, 19–21] or by dissociation of FM spin clusters (existing over a wide range of temperature) [18, 22–24, 27, 28]. In the present report, our attempt has been made to account for temperature dependences of the ESR linewidth and intensity $I(T)$ in a temperature range $T_L \le T < 500$ K, where T_L is summarized in Table 1.

According to the one-phonon process, the increase of ΔH with respect to temperature is linear, given by [19, 21]

$$\Delta H(T) = A + BT\,, \tag{2}$$

where A is a constant, and B is a parameter being related to lattice distortions. Having used Eq. (2) to fit the experimental data of $\Delta H(T)$, B was determined to be 5.45, 5.21, 4.98, 4.80, and 4.61 Oe/K for x = 0.1, 0.2, 0.3, 0.4, and 0.5, respectively, see Table 1. It can be seen that, in the temperature range in-

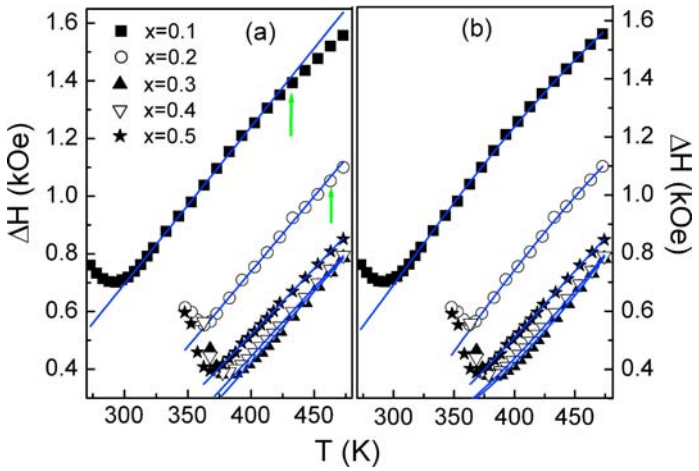

Fig. 3 (online colour at: www.pss-b.com) Temperature dependence of ΔH data for the samples. (a) ΔH data are fitted to the one-phonon relaxation process, Eq. (1); (b) ΔH data are fitted to the model of adiabatic hopping motion of small polarons, Eq. (3).

vestigated, B decreases with increasing the Pb-doped content, indicating a decrease of lattice distortions in the samples. As shown in Fig. 3(a), a deviation between the experimental and theoretical curves at 432 and 463 K, respectively, is observed for $x = 0.1$ and 0.2 compositions. This is related to a gradual transition from the bottleneck regime to the regime in that the rapid spin–lattice relaxation becomes comparable to the spin–spin relaxation [17, 19]. However, such behavior is not observed for $x \geq 0.3$ compositions. In fact, in the temperature region where Eq. (2) gives the best fit to the obtained $\Delta H(T)$ data, the Lande factor $g = \sim 2.0$ is temperature independent, meaning that spin–spin relaxations between the exchange couplings of Mn^{3+}–Mn^{4+} are predominate. For $x = 0.1$ and 0.2 compositions, an additional presence of the spin–lattice relaxation at high temperatures caused a slight reduction of g (see Fig. 4). In our system, the values of g were simply obtained using an equation [29, 34]

$$g = \frac{h\nu}{\mu_B H_r}, \tag{3}$$

where h, ν, and μ are the Planck constant, the microwave frequency, and the Bohr magneton, respectively. Obviously, one emerging question is what theoretical models can be used to explain $\Delta H(T)$ data in the temperature region where the spin–phonon coupling occurs strongly?

To clarify this, the temperature dependence of the ESR linewidth has been further investigated in the temperature region $T \geq T_L$. According to the model of adiabatic hopping motion of small polarons [4, 24], the $\Delta H(T)$ data can be described by the following expression

$$\Delta H(T) = \Delta H_0 + \frac{A'}{T} \exp\left(\frac{E_a}{k_B T}\right), \tag{4}$$

where k_B is the Boltzmann factor, ΔH_0 and A' are constants, and E_a is the thermal activation energy. The solid lines in Fig. 3(b) represent the best fit to Eq. (4) with activation energy values which denoted as E_{a1} in Table 1. Considering the model, the broadening of EPR spectra as increasing temperature is suggested to be related to the hopping rate of charge carriers that limited the lifetime of the spin state. As comparing to the one-phonon relaxation process, the adiabatic-hopping motion model of small polarons has been found to more suite to the $\Delta H(T)$ variation for our samples system, particularly for manganites containing lattice distortions [19, 24, 26] such as for the $x = 0.1$ and 0.2 samples. Accordingly, it is proposed that the hopping mechanisms [1, 2, 40, 41] of charge carriers for the $x \leq 0.2$ samples are different from those for the $x \geq 0.3$ samples, thereby causing the difference in the fitted-curves family, see Fig. 3(b).

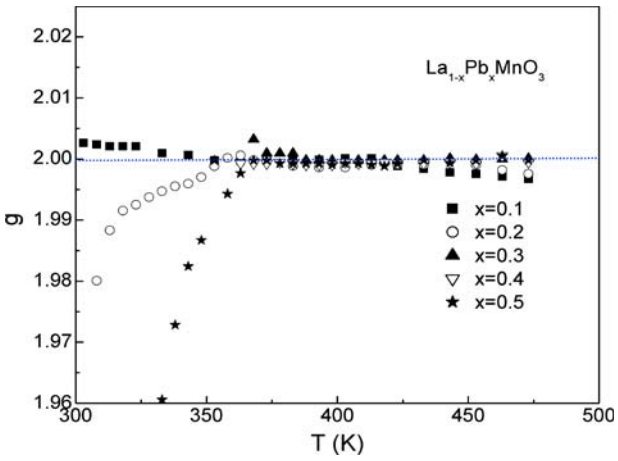

Fig. 4 (online colour at: www.pss-b.com) Temperature dependence of the effective g value for $La_{1-x}Pb_xMnO_3$ ($x = 0.1$, 0.2, 0.3, 0.4, and 0.5) compounds.

In an attempt to explain the temperature dependence of the ESR intensity, determined by numerical-double integration of measured spectra in the temperature region of $T \ge T_L$, we start with the one-phonon process. As proposed in Refs. [19, 35, 42], the ESR linewidth of a FM compound was given by:

$$\Delta H(T) = \frac{C}{T\chi(T)}[K(T) + f(\varepsilon)], \tag{5}$$

where C is the Curie constant and $\chi(T)$ is the susceptibility. $K(T)$ and $f(\varepsilon)$, with $\varepsilon = (T - T_C)/T_C$, represent the non-critical and critical contributions to $\Delta H(T)$, respectively. Assuming that no contributions to the linewidth from sources other than spin–spin interactions are present, C would be a temperature-independent value accordingly [36]. Furthermore, when $T \gg T_C$, $f(\varepsilon)$ is trivial and $K(T)$ goes to a constant [19, 42]. Considering such conditions, Eq. (4) can be re-written as

$$\Delta H(T) \propto \frac{C}{T\chi(T)}. \tag{6}$$

On the other hand, $I(T)$ is proportional to the susceptibility of the ions responsible for the ESR signal, i.e., $I(T) \propto \chi(T)$ [24, 27]. Combining this and Eq. (3), $I(T)$ is finally expressed by

$$I(T) = I_0 \exp\left(\frac{E_a}{k_B T}\right). \tag{7}$$

Figure 5(a) shows $I(T)$ data and fitting lines according to Eq. (7) for the samples. In this case, the activation energy E_a value (denoted as E_{a2}) was determined and summarized in Table 1. With the E_{a2} values given, the plot of ln (I/I_0) vs. T shows linear, as can be seen in Fig. 5(b). When considering the values of E_{a1} and E_{a2} obtained, respectively, from the ΔH_{pp} and $I(T)$ data, a deviation between these values has been found; this is probably due to ignoring a power function $f(\varepsilon)$ in the critical regime [37, 38].

Using the notification of $I(T) \propto \chi(T)$, it is possible to plot $1/I$ vs. T. As shown in Fig. 6(a), from the $1/I(T)$ curves for representative x = 0.1 and 0.5 compositions, the Curie–Weiss temperature, Θ, (see Table 1) was determined by extrapolating a linear-high-temperature part of the curve to zero value according to the Curie–Weiss law, $I(T) \propto 1/(T - \Theta)$ [17–19, 24, 25, 27]. We can see that the Curie–Weiss law does not well fit to the $I(T)$ data in a wide range of temperatures due to clustering FM spins near the Curie point [18, 20, 42]. It is therefore suggested that the appearance of the thermal activation energy

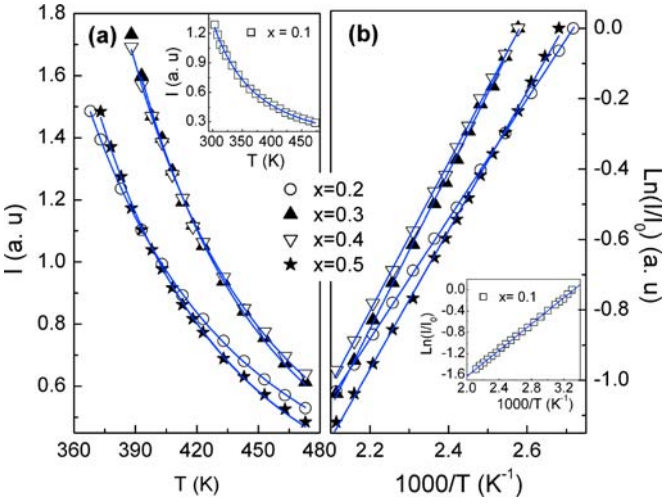

Fig. 5 (online colour at: www.pss-b.com) (a) Plot of $I(T)$ for the samples, the solid lines are fitting curves to Eq. (6). (b) The plot of ln (I/I_0) vs. 1000/T for the samples is fitted to a linear function.

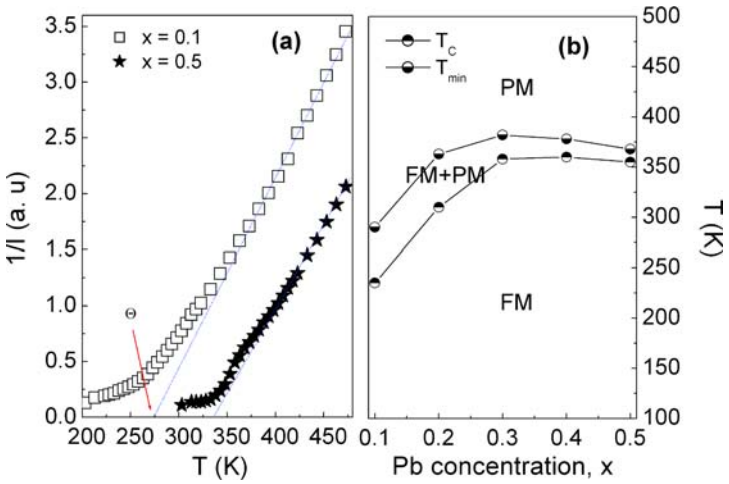

Fig. 6 (online colour at: www.pss-b.com) (a) Plot of $1/I(T)$ vs. T, dotted lines are fits to the Curie–Weiss law. (b) A magnetic phase diagram for $La_{1-x}Pb_xMnO_3$ (x = 0.1, 0.2, 0.3, 0.4, and 0.5) compositions. The FM and PM phases exist below T_C and above T_{min}, respectively, whereas in the temperature range of $T_C < T < T_{min}$ both these phases are coexistent.

which characterizes for the dissociation of FM clusters as increasing temperature is completely reasonable for such manganite perovskites.

To further understand the considering system, the changes in T_C (or T_{min}) and E_a are discussed in connection with those in the structure and mechanism interactions, when substituting La by Pb. It is shown that antiferromagnetic Mn^{3+}–Mn^{3+} super-exchange interactions plays a dominant role in a parent compound of $LaMnO_3$. Substitution of Pb for La leads to the appearance of Mn^{4+} ions, and consequently, FM double-exchange interactions between Mn^{3+} and Mn^{4+} ions introduce [39]. When the Pb-doped content increases from x = 0.1 to 0.3, the FM phase is enriched and become strongest at x = 0.3. Besides, it was found that the average bond length ⟨Mn–O⟩ of the system decreased (1.968, 1.966, and 1.962 Å for x = 0.1, 0.2, and 0.3, respectively) while the average bond angle ⟨Mn–O–Mn⟩ increased from 162° to 166° for x = 0.1 and 0.3, respectively [14]. These interpret why T_C (or T_{min}) and E_a increase with increasing the Pb-doped content. However, for further substitution of Pb ($x \geq 0.4$), T_C values of the samples remain unchanged or lightly decreased. This can be understood as an additional presence of AFM interactions of the super-exchange Mn^{4+}–Mn^{4+} coupling together with the pre-existing Mn^{3+}–Mn^{3+} coupling that are competing with the FM phase. The increase of E_a with the Pb addition even for the x = 0.4 and 0.5 compositions can be attributed to the changes in the structure of the samples. Because, unlike the $x \leq 0.3$ samples showing a rhombohedral structure, the x = 0.4 and 0.5 samples were found to have a cubic structure [7, 14], for which a higher value of the activation energy is often required to dissociate the FM clusters at temperatures $T > T_{min}$ [30]. It should be furthermore noted that the addition of Pb in $La_{1-x}Pb_xMnO_3$ led to a gradual increase in $\langle r_A \rangle$ from 1.032 (x = 0.1) to 1.116 Å (x = 0.5) [1, 2, 40].

Finally, a magnetic phase diagram of $La_{1-x}Pb_xMnO_3$ ($0.1 \leq x \leq 0.5$) compounds is displayed in Fig. 6(b). The FM and PM phases exist at temperatures below T_C and above T_{min}, respectively. In the intermediate temperature range, $T_C < T < T_{min}$, both FM and PM phases coexist. It can be seen from this phase diagram that $La_{1-x}Pb_xMnO_3$ materials would be promising candidates for the high-temperature applications.

4 Conclusions

The internal dynamics and magneto-transport properties in $La_{1-x}Pb_xMnO_3$ (x = 0.1, 0.2, 0.3, 0.4, and 0.5) compounds were thoroughly studied by means of ESR spectra. It was shown that the addition of Pb led

to a decrease in lattice distortions in the samples. The changes in the Curie temperature and activation energy are likely related to those in the structure and interaction mechanisms occurring within the samples. In terms of our experimental results, it is reasonable to indicate that the origin of ESR signals in the PM phase is due to the existence of ferromagnetic clusters over a wide range of temperature.

Acknowledgements This work was supported by the Korean Science and Engineering Foundation through the Research Center for Advanced Magnetic Materials at Chungnam National University.

References

[1] M. Ziese and M. J. Thornton, Spin Electronics (Springer-Verlag, Berlin, Heidelberg, 2001).
[2] T. A. Kaplan and S. D. Mahanti, Physics of Manganites (Kluwer Academic/Plenum Publishers, 1999).
[3] P. G. Radaelli, G. Iannone, M. Marezio, H. Y. Hwang, S.-W. Cheong, J. D. Jorgensen, and D. N. Argyriou, Phys. Rev. B **56**, 8265 (1997).
[4] C. W. Searle and S. T. Wang, Can. J. Phys. **47**, 2703 (1969); Can. J. Phys. **48**, 2023 (1970).
[5] S. F. Alvarado, W. Eib, P. Munz, H. C. Siegmann, M. Campagna, and J. P. Remeika, Phys. Rev. B **13**, 4918 (1976).
[6] K. P. Belov, E. P. Svirina, O. E. Portugal, M. M. Lukina, and V. I. Sotnikova, Sov. Phys. Solid State **20**, 2021 (1978).
[7] R. Mahendiran, R. Hahesh, A. K. Raychaudhuri, and C. N. R. Rao, J. Phys. D: Appl. Phys. **28**, 1743 (1995).
[8] Y. X. Jia, Li Liu, K. Khazeni, V. H. Crespi, A. Zettl, and M. L. Cohen, Phys. Rev. B **52**, 9147 (1995).
[9] I. O. Troyanchuk, D. D. Khalyavin, and H. Szymczak, Mater. Res. Bull. **32**, 1637 (1997).
[10] A. M. Niraimathi and M. Hofmann, Physica B **276–278**, 722 (2000).
[11] L. Ghivelder, R. S. Freitas, R. E. Rapp, F. A. B. Chaves, M. Gospodinov, and M. A. Gusmao, J. Magn. Magn. Mater. **226–230**, 845 (2001).
[12] A. Banerjiee, B. K. Chaudhuri, A. Sarkar, D. Sanyal, and D. Banerjiee, Physica B **299**, 130 (2001).
[13] Y. Yamada, T. Kusumori, and H. Muto, Appl. Phys. Lett. **80**, 1409 (2002).
[14] N. Chau, H. N. Nhat, N. H. Luong, D. L. Minh, N. D. Tho, and N. N. Chau, Physica B **327**, 270 (2003).
[15] S. Pal, B. K. Chaudhuri, S. Neeleshwar, Y. Y. Chen, and H. D. Yang, J. Appl. Phys. **97**, 043707 (2005).
[16] S. E. Lofland, S. M. Bhagat, H. L. Ju, G. C. Xiong, T. Venkatesan, and R. L. Greene, Phys. Rev. B **52**, 15058 (1995).
[17] A. Shengelaya, G. M. Zhao, H. Keller, and K. A. Muller, Phys. Rev. Lett. **77**, 5296 (1996).
[18] S. B. Oseroff, M. Torikachvili, J. Singley, A. Ali, S.-W. Cheong, and S. Schultz, Phys. Rev. B **53**, 6521 (1996).
[19] C. Rettori, D. Rao, J. Singley, D. Kidwell, S. B. Oseroff, M. T. Causa, J. J. Neumeier, K. J. McClellan, S.-W. Cheong, and S. Schultz, Phys. Rev. B **55**, 3083 (1997).
[20] S. E. Lofland, P. Kim, P. Dahiroc, S. M. Bhagat, S. D. Tyagi, S. G. Karabashev, D. A. Shulyatev, A. A. Arsenov, and Y. Mukovskii, Phys. Lett. A **233**, 476 (1997).
[21] C. Oliva, L. Forni, P. Pasqualin, A. D'Ambrosio, and A. V. Vishniakov, Phys. Chem. Phys. **1**, 355 (1999).
[22] A. I. Shames, E. Rozenberg, G. Gorodetsky, B. Revzin, D. Mogilyanski, J. Pelleg, and I. Felner, J. Magn. Magn. Mater. **203**, 259 (1999).
[23] D. L. Huber, G. Alejandro, A. Caneiro, M. T. Causa, F. Prado, M. Tovar, and S. B. Oseroff, Phys. Rev. B **60**, 12155 (1999).
[24] A. Shengelaya, G. M. Zhao, H. Keller, K. A. Muller, and B. I. Kochelaev, Phys. Rev. B **61**, 5888 (2000).
[25] R. Gupta, J. P. Joshi, S. V. Bhat, A. K. Sood, and C. N. R. Rao, J. Phys.: Condens. Matter **12**, 6919 (2000).
[26] S. B. Oseroff, N. O. Moreno, P. G. Pagliuso, C. Rettori, D. L. Huber, J. S. Gardner, J. L. Sarrao, J. D. Thompson, M. T. Causa, G. Alejandro, M. Tovar, and B. R. Alascio, J. Appl. Phys. **87**, 5810 (2000).
[27] A. N. Ulyanov, S. C. Yu, S. G. Min, and G. G. Levchenko, J. Appl. Phys. **91**, 7926 (2002).
[28] S. Angappane, G. Rangarajan, and K. Sethupathi, J. Appl. Phys. **93**, 8334 (2003).
[29] A. Abragam and B. Bleaney, Electron Paramagnetic Resonance of Transiton Ions (Oxford University Press, 1993).
[30] T. L. Phan, N. V. Khiem, J. Zidanic, N. X. Phuc, and S. C. Yu, IEEE Trans. Magn. **41**, 2769 (2005).
[31] N. A. Viglin, S. V. Naumov, and Ya. M. Mukovskii, Phys. Solid State **43**, 1934 (2001).
[32] A. Carrington and A. D. McLachlan, Introduction to Magnetic Resonance (Chapman and Hall, London–New York, 1980), p. 10.

[33] L. Pi, X. Xu, and Y. Zhang, Phys. Rev. B **62**, 5667 (2000).
L. Pi, L. Zheng, and Y. Zhang, Phys. Rev. B **61**, 8917 (2000).
[34] K. W. Joh, C. H. Lee, C. E. Lee, and Y. H. Jeong, phys. stat. sol. (b) **239**, 452 (2003).
[35] D. L. Huber and M. S. Seehra, J. Phys. Chem. Solids **36**, 723 (1975).
[36] A. G. Plores, V. Raposo, J. Iniguez, S. B. Oseroff, and C. de Francisco, J. Magn. Magn. Mater. **226–230**, 574 (2001).
[37] T. G. Castner, Jr. and Mohindar S. Seehra, Phys. Rev. B **4**, 38 (1971).
[38] B. I. Kochelaev, L. Kan, B. Elschner, and S. Elschner, Phys. Rev. B **49**, 13106 (1994).
[39] C. Zener, Phys. Rev. **82**, 403 (1951).
[40] J. Rubio O. and C. Marin, J. Phys. C: Solid State Phys. **20**, 1173 (1987).
[41] T. L. Phan, N. D. Tho, M. H. Phan, N. D. Ha, N. Chau, and S. C. Yu, Physica B **371**, 317 (2006).
[42] S. Angappane, M. Pattabiraman, G. Rangarajan, and K. Sethupathi, J. Appl. Phys. **97**, 10H705 (2005).